A Genome-Wide Association Study of Non-Photochemical Quenching in response to local seasonal climates in *Arabidopsis thaliana*

Authors

Tepsuda Rungrat[1,2,*], Andrew A. Almonte[2,*], Riyan Cheng[3], Peter J. Gollan[4], Tim Stuart[5], Eva-Mari Aro[4], Justin O. Borevitz[2], Barry Pogson[2] and Pip B. Wilson[2,†]

[1]Faculty of Agriculture, Natural resources and Environment, Naresuan University, Thailand; [2]ARC Centre of Excellence for Plant Energy Biology, Australian National University, Canberra, Australia; [3]Department of Psychiatry, University of California San Diego, La Jolla, CA 92093, USA; [4] Faculty of Engineering and Science, University of Turku, Turku, Finland; [5]ARC Centre of Excellence for Plant Energy Biology, University of Western Australia, Perth, Australia

* These authors contributed equally to this work

† Corresponding author: pipbwilson@gmail.com

Abstract

Field-grown plants have variable exposure to sunlight as a result of shifting cloud-cover, seasonal changes, canopy shading, and other environmental factors. As a result, they need to have developed a method for dissipating excess energy obtained from periodic excessive sunlight exposure. Non-photochemical quenching (NPQ) dissipates excess energy as heat, however the physical and molecular genetic mechanics of NPQ variation are not understood. In this study, we investigated the genetic loci involved in NPQ by first growing different *Arabidopsis thaliana* accessions in local and seasonal climate conditions, then measured their NPQ kinetics through development by chlorophyll fluorescence. We used genome-wide association studies (GWAS) to identify 15 significant quantitative trait loci (QTL) for a range of photosynthetic traits, including a QTL co-located with known NPQ gene *PSBS* (AT1G44575). We found there were large alternative regulatory segments between the *PSBS* promoter regions of the functional haplotypes and a significant difference in PsbS protein concentration. These findings parallel studies in rice showing recurrent regulatory evolution of this gene. The variation in the *PSBS* promoter and the changes underlying other QTLs could give insight to allow manipulations of NPQ in crops to improve their photosynthetic efficiency and yield.

B.P. & J.B. conceived the project; B.P., J.B., P.W. and T.R. designed the research plan and analysis; P.W. supervised the experiments; T.R. performed most of the experiments and analysis; P.G., T.S., A.A. & E.A. designed and undertook experimental design, experiments and analysis for Figure 4; R.C. did the GWAS analysis; P.W., T.R. & A.A. wrote the article with contributions of all the authors.

Keywords: GWAS, Arabidopsis, photoprotection, natural variation, acclimation

INTRODUCTION

Photosynthesis is the process of harnessing light energy to power CO_2 fixation. Variability in light environments of a plant or leaf caused by clouds or canopy shading can often result in rapid switching between limited or excess light exposure in relation to the acclimated state. Excess light can result in the production of damaging reactive oxygen species, which can impair leaf photosynthesis even after return to low light. Plants have evolved a method to dissipate excess light energy from the major light-harvesting antennae as heat through a photoprotective mechanism known as non-photochemical quenching (NPQ; Reviewed in Ruban, 2016). This process can eliminate over 75% of absorbed light energy (Niyogi, Grossman, & Bjorkman, 1998) and modified regulation of NPQ has been shown to improve photosynthetic efficiency and increase biomass in field-grown tobacco (Kromdijk et al., 2016).

In vascular plants, the NPQ mechanism is generally classified into two main components: energy-dependent quenching (qE) and photoinhibition quenching (qI; Ruban, 2016). qE is recognized as the most significant component of NPQ and can be rapidly increased and relaxed within seconds to minutes. qE is triggered by a decrease in the thylakoid lumen pH (Briantais, Vernotte, Picaud, & Krause, 1979), which induces thermal dissipation through protonation of the PsbS protein, as well as the serial de-epoxidation of violaxanthin to antheraxanthin and then zeaxanthin through the xanthophyll cycle (Reviewed in Demmig-Adams & Adams, 1992; Jahns & Holzwarth, 2012). Conformational changes in the light-harvesting antennae activated during qE involve monomerization of PsbS (Correa-Galvis, Poschmann,

72 Melzer, Stuhler, & Jahns, 2016; X. P. Li et al., 2004); however, the precise role of
73 PsbS in the dissipation of excess energy is as yet unclear.
74
75 The worldwide Arabidopsis collection contains natural diversity in a range of traits
76 that have resulted from adaptation to a wide range of climate types, and significant
77 variation in NPQ was observed in a study of 62 diverse Arabidopsis accessions
78 (Jung & Niyogi, 2009). The mapping of biparental populations from contrasting
79 accessions has identified several novel loci involved in NPQ, including reinforcing
80 the role of *PSBS* (Jung & Niyogi, 2009). However, to our knowledge, no studies have
81 undertaken genome wide association studies (GWAS) on NPQ in Arabidopsis.
82 GWAS surveys a much wider range of genetic diversity than bi-parental populations
83 and also provides greater resolution for mapping quantitative trait loci (QTL) to assist
84 in gene discovery. The utility of GWAS for NPQ has already been demonstrated
85 through the characterization of 33 QTL in rice (Wang et al., 2017) and 15 QTL in
86 soybean (Herritt, Dhanapal, & Fritschi, 2016).
87
88 The use of high-throughput phenotyping platforms that measure photoprotective
89 traits using chlorophyll fluorescence have proven to be useful methods for monitoring
90 real-time plant stress responses in model species such as Arabidopsis (Rousseau et
91 al., 2013; Rungrat et al., 2016; van Rooijen, Aarts, & Harbinson, 2015). Phenotyping
92 platforms such as PlantScreen can measure large numbers of plants simultaneously
93 to reveal the photosynthetic performance of whole rosettes. Additionally, modified
94 growth chambers can be used to precisely mimic external climates (Brown et al.,
95 2014) without the noise of field conditions, facilitating the assessment of the impact
96 of genetic variations on responses to even minor environmental variation. Combined

with the extensive genetic resources available for Arabidopsis (1001 Genomes Consortium, 2016; Y. Li, Huang, Bergelson, Nordborg, & Borevitz, 2010; Zhang, Hause, & Borevitz, 2012), these tools enable the dissection of the genetic architecture underlying important photoprotective traits such as NPQ and their response to different environmental conditions.

In this study, we focus on identifying the effect of contrasting climates (in the form of differing light intensities and temperature profiles) on the kinetics of NPQ in several Arabidopsis accessions from the global diversity set. We then use GWAS to reveal the genetic basis underlying NPQ and its response to the environment. With these methods, we aim to better understand the genetic framework of this important physiological pathway in its response to excess light energy that occurs in natural environments.

MATERIAL AND METHODS

Plant growth

For GWAS, 284 genetically diverse Arabidopsis accessions were selected from the global HapMap set (Y. Li et al., 2010). Two photoprotective mutants (*npq1* and *npq4*; Y. Li et al., 2010; Niyogi et al., 1998) were included as controls for reduced NPQ. *npq1* is a loss of function mutant in violaxanthin de-epoxidase 1 (VxDE; AT1G08550) while *npq4* is a loss of function mutant in *PSBS* (AT1G44575). Most accessions had one replicate per environmental condition while 16 replicates of Col-0 were included in each condition to monitor the extent of spatial variation within the chamber and four replicates of *npq4* were included in the late autumn conditions. Seed germination was synchronised by stratification at 4^{o}C in the dark in sterilised water

for 4-5 days. Plants were grown in pots (4 cm x 4 cm x 7 cm) of pasteurised seed raising mix (Debco seed raising mix, Scotts Australia) without further fertilisation in specially modified climate chambers (Brown et al., 2014) housed in the plant growth facility of the Australian Plant Phenomics Facility at the ANU. These chambers have been fitted with 7-bands LED light panels and are programmed to alter light intensity, light spectrum, air temperature and relative humidity every 5 minutes. Climatic conditions were modelled using SolarCalc software (Spokas & Forcella, 2006). In this study, two experiments were run with diurnal and seasonal temperature fluctuations with two climates in each experiment set to simulate coastal (Wollongong: -34.425, 150.893) and inland (Goulburn: -34.426, 150.892) regions of South East Australia. The first experiment was conducted by simulating a typical late-autumn season starting from April 1st, 2014 and ending on June 5th, 2014. The second experiment was conducted to simulate an early autumn season, starting from March 15th, 2015 and finishing on May 7th, 2015. The maximum light intensity at noon was around 150 µmol photons $m^{-2}s^{-1}$ and 300 µmol photons $m^{-2}s^{-1}$ for Coastal and Inland, respectively, in both experiments. These are typical light intensities for growing *Arabidopsis thaliana* (Bölter, Seiler, & Soll, 2018). The temperature ranged between 14ºC - 23ºC and 10ºC - 23ºC for Coastal-Late Autumn and Inland-Late Autumn respectively, and these temperatures decreased to 10ºC - 18ºC and 5ºC - 15ºC by the end of the experiment due to seasonal change to winter. The temperature ranged between 10ºC - 25ºC and 5ºC - 25ºC for Coastal-Early Autumn and Inland-Late Autumn respectively, and these temperatures decreased to 10ºC - 18ºC and 5ºC - 18ºC by the end of the experiment due to seasonal change to winter.

NPQ quantification by chlorophyll fluorescence measurement

Photosynthesis parameters were measured by pulse amplitude modulation chlorophyll fluorescence using the automated PlantScreen system (Photon Systems Instruments, Czech Republic) when plants were at 25 and 40 days of age and at 14 and 16 leaves stages. All measurements began at midday and finished by 5:00 pm. Chlorophyll fluorescence kinetics were monitored during illumination of actinic light (700 µmol $m^{-2}s^{-1}$) and saturation flashes (800ms, 2800 µmol $m^{-2}s^{-1}$) and analysed using FluorCam7 software. To focus on the major qE component, a custom-made chlorophyll fluorescence measurement protocol was used (P3; Rungrat et al., 2016). After 30 minutes dark adaptation, F_o was measured in the dark before F_m was measured with an initial saturating pulse in the dark, followed by a series of saturating pulses 60 seconds apart to monitor F_m' and F' during the 8 minutes of actinic light illumination and following 3 minutes dark relaxation period. NPQ can be calculated from the ratio of change in F_m and F_m' during the illumination as shown in the equation:

$$NPQ = (F_m - F_m')/F_m' \quad \ldots\ldots\ldots\ldots\ldots\ldots (1)$$

with F_m' and F_m being the maximal fluorescence of the light-adapted and dark-adapted leaf, respectively. In addition to NPQ, dark adapted F_v/F_m (QY-max) was measured as an indicator of photoinhibition and light adapted F_v'/F_m' was the measure of photosynthetic efficiency under the actinic light.

Statistical analysis and QTL mapping

Experimental Design

Our goal is to identify quantitative trait loci as associated SNPs underlying photoprotection traits. In genome wide association studies (dominated by human genetics) the level of replication is at the level of the SNP, which ideally would be independent of other loci. Because of both local linkage disequilibrium and background population structure SNPs are not independent. This is particularly true with inbred accessions. Fortunately, a large collection of accessions is available which were selected to be roughly equidistantly related to each other (Platt et al, 2010). Thus, to maximise statistical power for identifying genetic variants underlying phenotypes, a panel of 284 natural accessions of Arabidopsis was selected from the HapMap collection for the Late Autumn experiment and an overlapping panel of 223 accessions was selected for the Early Autumn experiment. To maximize the number of accessions within an experiment, single replicates were grown in each climate condition. The Col-0 accession was replicated 16 times to allow calculation of biological variation of the traits.

For the phenotypic data, three phases of NPQ kinetics were examined. Induction was determined by NPQ formation when actinic light illumination was initiated, followed by a steady state phase and lastly, a relaxation phase in the dark (induction: 0 - 120 sec, steady state: 120 - 450 sec, and relaxation phases: 450 - 610 sec, Fig 2). The rate of induction was calculated as average slope of increase in NPQ during the induction (0 - 120 seconds); the maximum NPQ value was determined as the maximum value reached throughout the whole experiment and the rate of relaxation was calculated as the average slope during the dark relaxation (450 - 610 seconds). As relatively few, equally spaced, time points were sampled during NPQ, fitting nonlinear induction and relaxation kinetics is unlikely to change the results

196 substantially. This is because the QTL effect is not the kinetics of particular
197 accession, but the relative difference between summaries of the kinetic paths among
198 SNP genotypes (Fig1).
199
200 The individual phenotypes for each accession was used for the GWAS separately in
201 both climate conditions. To determine the GxE interaction, all data was used in a
202 single GWAS and each SNPs was tested for a main and climate specific effect and
203 relatedness among accessions was accounted for as a random effect kinship matrix
204 (Li et al, 2014). SNP data from the 6M SNPs data set (1001 Genomes Consortium,
205 2016) was filtered for a minor allele frequency <2.5% with a final set of
206 approximately 1.7 million SNPs. GWAS were performed using the R package
207 QTLRel (R. Cheng, Abney, Palmer, & Skol, 2011), based on model (2) below, which
208 incorporated a relationship matrix to correct for confounding population structure.
209
210 $$y = x + z + u + \epsilon \qquad \ldots\ldots\ldots\ldots\ldots\ldots (2)$$
211
212 where $y = (y_{ij})$ is a vector of the n phenotypic values with y_{ij} being the j-th accession
213 in the i-th environment (i.e. one of the two climate conditions within each
214 experiment), $x = (x_{ijk})_{nx(K+1)}$ represents the intercept and k covariates (if any) with
215 effects β, z is a vector of the coded genotypes at a scanning locus with effect γ, u =
216 $(u_1, u_2, \ldots\ldots, u_n)'$ represents polygenic variation, and $\epsilon = (\epsilon_1, \epsilon_2, \ldots\ldots, \epsilon_n)$ the residual
217 effect. It was assumed that $u \sim N(0, G\sigma_g^2)$, $\epsilon \sim N(0, I\sigma^2)$ and u was independent of ϵ.
218 The genetic relationship matrix G was estimated by identify-by-state (IBS) from
219 genotypic data with markers on the chromosome under scan being excluded to avoid
220 proximal contamination (Riyan Cheng, Parker, Abney, & Palmer, 2013; Listgarten et

al., 2012). A 0.05 genome-wide significance threshold was determined by the Bonferroni procedure, i.e., 2(1-0.05/m,1), where m is the number of SNPs. This threshold turned out to be very close to empirical thresholds estimated by the permutation test.

Visualisation of alignments between KBS-Mac-74 and Col-0 accessions

Kablammo (Wintersinger & Wasmuth, 2015) was used to obtain a graphical understanding of the alignments between the *PSBS* genomic regions of the TAIR 10 Col-0 reference genome (Chr1: 16,866,832..16,873,428) and the recently sequenced KBS-Mac-74 genome (Michael et al., 2018). The sequence for the Col-0 *PSBS* genomic fragment was downloaded from the 1001 genomes project website and the KBS-Mac-74 genome was available on the European Nucleotide Archive (1001 Genomes Consortium, 2016; Michael et al., 2018). The KBS-Mac-74 genome was aligned with the Col-0 genomic fragment using Sequence Server v1.0.9 (Priyam et al., 2015) and the results were uploaded onto and visualised with Kablammo.

Alignment of reads to Col-0 and KBS-Mac-74 haplotypes

Paired-end sequence reads for high and low NPQ accessions sequenced as part of the 1001 Genomes Project (1001 Genomes Consortium, 2016) were downloaded from NCBI SRA and trimmed for adapter content and low quality bases using Trimmomatic v0.36 (Bolger, Lohse, & Usadel, 2014) with the following parameters: LEADING:3 TRAILING:3 SLIDINGWINDOW:4:15 MINLEN:36. Retained paired-end reads were aligned to the Col-0 and KBS-Mac-74 genomes separately using Bowtie2 local alignment (1 mismatch per seed, maximum of 5 re-seeds; (Langmead & Salzberg, 2012). Alignment files were sorted and indexed using samtools (H. Li et

al., 2009). Read coverage tracks were created for each accession using deepTools bamCoverage, with the coverage normalized to the number of reads per kilobase per million mapped reads (Ramirez et al., 2016). Coverage information around the *PSBS* genomic region was extracted from bedgraph files using bedtools v2.25 (Quinlan & Hall, 2010).

Semi-quantification of PsbS protein in high and low NPQ lines

Five accessions with high NPQ and five accessions with low NPQ (Supplemental 6), as well as the *npq4* mutant and *PSBS* over-expression line, were grown for 6 weeks in 8 h day/16 h night cycle under 150 µmol photons $m^{-2}s^{-1}$ light with a temperature range of 8.6 °C – 18 °C. Mature leaves from 4 – 6 plants were pooled, frozen in liquid nitrogen, ground to a powder, and total proteins were extracted in 20 mM Tris-HCL solution (pH 7.8) containing 2 % SDS and protease inhibitor. After incubation at 37 °C and centrifugation, protein concentrations in the supernatants were measured using the Lowry assay. For each sample, 10 µg total protein were separated on SDS-PAGE gels containing 15% acrylamide, then transferred to PVDF membranes and blotted with a polyclonal antibody specific to the PsbS protein (a gift from R. Barbato). Six replicate Western blots containing all samples were developed and antibody signal intensities were quantified using an Odyssey CLx Imaging System (LI-COR). PsbS signals were normalised against a second non-specific protein band that was equally present in all samples (see Supplemental data). Statistical significance between the normalised signals was determined by a paired Student's T test (N=30).

RESULTS

Natural variation of NPQ in Arabidopsis accessions in response to different climatic conditions

To determine the characteristics of NPQ in stressful environments, an Arabidopsis HapMap population of 284 accessions was grown in modified climate chambers (Brown et al., 2014) programmed to simulate contrasting environments: a “coastal” environment representing a temperate climate with light intensities similar to conditions conventionally used to grow Arabidopsis, and an “inland” environment representing a larger temperature range and higher light intensities (Supplemental 1). Two experiments were run with each condition starting at early- or late-autumn and transitioning into winter. There were clear differences in growth and development within the Arabidopsis HapMap population between the two conditions in both experiments (Fig 1A and B) as plants grown in inland conditions grew smaller than their coastal counterparts. Due to this variation in growth rate, environmental effects on NPQ phenotypes were measured when the Col-0 control plants reached a similar developmental stage (i.e. 14 or 16 leaves) rather than after a predefined period post-germination.

The NPQ kinetics of the plants showed variation dependent on their growth conditions and the developmental stage at which they were measured. When the samples were measured at the 14-leaf stage, plants grown in inland early-autumn conditions had a moderately faster NPQ induction relative to plants grown in coastal conditions by approximately 54%. However, the same plants grown in coastal and inland late-autumn conditions displayed largely similar NPQ kinetics (Fig 1C and D). All 14-leaf plants showed a rapid induction of NPQ that lasted approximately 1.5 – 2 minutes after exposure to actinic light (700 μmol $m^{-2}s^{-1}$), although plants grown in

296 early-autumn conditions reached a maximum NPQ followed by a moderate decline
297 throughout illumination (Fig 1C). In contrast, NPQ in plants grown in late-autumn
298 conditions continued to increase during actinic light exposure (Fig 1D). Additionally,
299 plants grown in late-autumn conditions reached a higher overall NPQ and returned
300 more rapidly to basal levels during dark incubation following actinic light exposure.
301
302 NPQ kinetic profiles showed a dramatic difference between plants grown in coastal
303 and inland conditions when measured at the 16-leaf growth stage (Fig 1E and F).
304 Both groups had a rapid induction of NPQ within approximately 1.5 – 2 minutes of
305 exposure to actinic light, though plants grown in coastal conditions were slightly
306 slower to reach a steady phase. After the initial induction of NPQ upon actinic light
307 exposure, plants grown in inland conditions reached their maximum average NPQ
308 within 2 minutes, followed by a moderate and steady decrease in NPQ during
309 illumination. Plants grown in coastal conditions continued to slowly increase during
310 the same period before reaching their maximum NPQ after 7.5 minutes of
311 illumination and directly before being transferred into darkness.
312
313 Of the plants grown to the 16-leaf stage, those grown in early-autumn conditions
314 showed a larger variance in NPQ (Fig 1E – F). Inland plants measured in early-
315 autumn achieved a maximum average NPQ of 2.47 (s.d. 0.38) after two minutes of
316 exposure to actinic light, while coastal plants achieved a maximum average NPQ of
317 2.89 (s.d. 0.39) after five minutes of exposure. Plants measured in late-autumn
318 conditions showed an overall higher NPQ, as inland plants achieved a maximum
319 average NPQ of 2.62 (s.d. 0.88) after two minutes exposure to actinic light, while
320 coastal plants achieved the highest NPQ average of 3.24 (s.d. 0.78) after 7.5

minutes of exposure to actinic light. When moved to darkness, the plants from inland conditions exhibited faster NPQ relaxation than plants grown in coastal conditions.

Photoprotective mutants *npq1*, lacking VxDE (Niyogi et al., 1998) and *npq4*, lacking PsbS (X. P. Li et al., 2000) were included as controls in all NPQ measurements. The mutants exhibited approximately four times lower steady-state NPQ than all wild-type accessions in both inland and coastal conditions and exhibited almost no NPQ relaxation (Fig 1C – F).

Genome-wide association identifies 15 significant QTL for NPQ kinetics

In order to gain a better understanding of the QTL involved in NPQ, a GWAS was conducted using the R package QTLRel (R. Cheng et al., 2011) and the 6M SNP marker set (1001 Genomes Consortium, 2016). For mapping, a number of derived traits were calculated at both the 14- and 16-leaf stages, including the rate of NPQ induction, the slope of the steady phase, maximum NPQ value, and the rate of NPQ relaxation (Fig 2). For the late-autumn experiment, six QTL were identified across the three kinetic parameters of NPQ production, including QTL5-3 for the Genotype x Environment (GxE) interaction between the two conditions (Table 1, Fig 2H). For the early-autumn experiment, eight QTL were identified across the three kinetic parameters of NPQ production, including QTL2-3 and QTL4-1 for the GxE interaction. Interestingly, none of the NPQ QTL were identified in both experiments or in any two conditions. Mapping of the photosynthetic traits F_v/F_m‘ and QY-max under all conditions revealed five QTL, including QTL1-4 and QTL2-2 previously identified as NPQ QTL. The majority (12/15) of QTL were identified at the 16-leaf

345 developmental stage, with only QTL2-2 being identified at both developmental
346 stages but for different traits.
347
348 These QTL were investigated in the TAIR database (Table 1; Huala et al., 2001), but
349 a majority were not associated with an obvious candidate gene. QTL1-4 was a
350 strong QTL identified in the coastal late-autumn condition for the slope of the steady
351 phase and rate of NPQ relaxation (Fig 2C – D), as well as F_v/F_m and maximum NPQ
352 value (Table 1). It was also associated with QY-max in the inland late-autumn
353 condition where it was slightly below the significance threshold. The SNP with the
354 highest logarithm of odds (LOD) score for QTL1-4 was located in the promoter of the
355 candidate gene *photosystem II subunit S* (*PSBS*; AT1G44575; Fig 3).
356
357 **Sequence variation in the PsbS promoter indicates differential induction of**
358 ***PSBS* that may be important in NPQ regulation**
359 To explore a possible relationship between natural variation in the *PSBS* genomic
360 region and the diversity in NPQ phenotypes, the SNP-corrected sequences of the
361 ten highest and ten lowest NPQ accessions determined in this experiment were
362 acquired from the 1001 genomes project (Supplemental 1B; Weigel & Mott, 2009).
363 Four SNPs were identified in the PsbS coding region in a comparison between the
364 two haplotype groups (low NPQ and high NPQ), although each of these encoded
365 synonymous amino acid residues (Supplemental 1A). Nevertheless, as these are
366 SNP-corrected sequences, there may be major insertions or deletions that may not
367 have been identified.
368

To compare the sequences of the high and low NPQ accessions, the raw reads of the *PSBS* genomic region from the 1001 genomes project were aligned to both the Col-0 reference genome (TAIR 10) and the recently sequenced KBS-Mac-74 genome (Michael et al., 2018). KBS-Mac-74 was chosen because it was the only accession available with long-read genomic sequence data and has not been SNP-corrected. Seven of the ten high NPQ accessions were available in the 1001 genomes project and all seven showed the same pattern of missing sections in the alignments to the promoter of *PSBS* to the Col-0 reference but aligned well to the KBS-Mac-74 genome. Similarly, of the eight low NPQ accessions available, all eight aligned well to the Col-0 reference but had missing sections in the alignment to the *PSBS* promoter from the KBS-Mac-74 genome (Fig 4A – D). When the Col-0 and KBS-Mac-74 genomes were aligned at this region there were two sections in the promoter of *PSBS* that did not align. One section was 1,251 bp in Col-0 corresponding with 691 bp in KBS-Mac-74, and the other was 100 bp in Col-0 corresponding with 3,000 bp in KBS-Mac-74 (Fig 4E).

To determine if there was a difference in PsbS protein abundance between high and low NPQ accessions, PsbS protein was quantified by Western blotting. Five plants representative of each NPQ haplotype were grown for six weeks under coastal late-autumn conditions. A small but highly significant difference in PsbS abundance between the two haplotype groups was identified (Fig 4F), with the high NPQ haplotype plants producing ~30% higher amounts of PsbS on average.

DISCUSSION

393 In this study, climate chambers were used to investigate the effect of local seasonal
394 growing conditions on the non-photochemical quenching (NPQ) pathway. A genome-
395 wide association study (GWAS) was used to investigate the genetic architecture of
396 NPQ and determine what quantitative trait loci (QTL) are involved in this
397 physiological process, as it is important for high light tolerance.
398
399 It was clear that different climate conditions affected growth, as plants grown in
400 coastal conditions grew larger than their inland cohort. The inland environment was
401 programmed to provide higher light intensities and lower temperatures than the
402 coastal environment, so NPQ would be more active in plants grown in inland
403 conditions. Leaf expansion is inversely correlated with light intensity (Potter, Rood, &
404 Zanewich, 1999) and content of the plant hormone gibberellic acid, which may
405 underlie why plants grown in high-light environments are physically smaller
406 (Reviewed in Hedden & Sponsel, 2015; Stowe & Yamaki, 1957).
407
408 The NPQ kinetic profiles of the plants in this study were found to be influenced by
409 development and climate conditions. When grown to the 14-leaf stage, there was
410 little difference in the NPQ kinetic profiles between plants grown in either inland or
411 coastal climates. However, their NPQ profiles changed dramatically when grown to
412 the 16-leaf stage. Despite these changes, there were some commonalities. For
413 example, plants grown in inland conditions had consistently faster induction of NPQ
414 when exposed to actinic light, which suggests the relatively more stressful growing
415 environment has primed these plants to more rapidly respond to stressful conditions.
416 Furthermore, all plants in all conditions rapidly resolved their NPQ when moved to
417 darkness, though inland-grown 16-leaf plants did so more quickly. The steady

418 decrease in NPQ observed in the inland-grown 16-leaf plants during their exposure
419 to actinic light also suggests they are better acclimated to utilise abiotic stress
420 response pathways. Differences in glutathione content between inland- and coastal-
421 grown plants may be a potential mechanism for this observation as glutathione is a
422 potent antioxidant that fluctuates with light intensity (Alsharafa et al., 2014).
423 However, more research must be done to confirm this. The differences in NPQ
424 kinetic profiles between plants grown under field-simulating high- and low-light
425 environments demonstrates how dynamic environments can condition plants to
426 develop appropriate physiological adaptations. Genetic variation in this response
427 may underlie such adaptations to the particular light environments where the plants
428 were collected.
429
430 To determine the genetic architecture of NPQ, a GWAS was performed and a total of
431 15 QTL were found to be involved in different components of NPQ (Table 1). They
432 were detected across different developmental stages and different seasonal climatic
433 conditions. The majority were found in the 16-leaf stage, further implying the
434 relevance of plant development in local seasonal climates on NPQ efficiency.
435 Arabidopsis has a wide geographic distribution and each accession would
436 experience different conditions in their native environments. This variation was
437 revealed through QTL that varied between the two simulated environments. All 15
438 QTL identified were associated with multiple candidate genes (Supplemental 7). For
439 example, QTL1-5 may be associated with *NDF5*, a gene involved in regulation of
440 gene expression and electron transport in photosystem I (Ishida et al., 2009). QTL5-
441 2 may be associated with *PTST*, which encodes a chloroplast-localised protein that
442 is involved in protein translocation (Lohmeier-Vogel et al., 2008).

QTL1-4 is the most prominent QTL identified in this study and is associated with *PSBS*, a gene known to be involved with NPQ (X. P. Li et al., 2000). The exact role of the PsbS protein in the NPQ pathway is currently unclear. It has been found to bind to chlorophylls and xanthophylls, making it the possible site of xanthophyll-dependent NPQ (X. P. Li et al., 2000). PsbS has also been found to induce conformational changes in the antennae of photosystem II (Horton, Wentworth, & Ruban, 2005). Regardless, PsbS is known to be a requirement because *npq4* is a PsbS loss-of-function mutant and consequently shows little to no NPQ activity (X. P. Li et al., 2000).

This study also found evidence for a correlation between NPQ competency and the *PSBS* genomic architecture. Gene alignments were performed for the highest and lowest NPQ accessions, with TAIR 10 Col-0 and KBS-Mac-74 (Michael et al., 2018) being the models for low and high NPQ accessions, respectively (Fig 4). These alignments show little variation within the protein-coding regions of *PSBS*, which ultimately have no impact on protein function since they do not alter the amino acid sequence. Alignments of the *PSBS* genomic regions from high and low NPQ accessions show structural variation within the promoter elements of the *PSBS* gene. The non-homologous elements may be due to a deletion, transposition, and/or a gene conversion event. There did not appear to be any obvious regulatory elements within those promoter regions, though more experimentation and functional tests would be required to determine their precise effect on PsbS expression and NPQ. Regardless, there does appear to be a significant influence on PsbS protein

467 expression as high NPQ accessions have a relatively higher level of leaf PsbS
468 protein content when grown in coastal late-autumn conditions (Fig 4F).
469
470 Besides genotypic and phenotypic variations in NPQ, there are also several
471 instances of genotype-by-environment (GxE) interaction, mostly in NPQ induction.
472 As previously mentioned, this may be due to plants grown in high-light environments
473 being better conditioned to respond to light stress. QTL2-3 and QTL5-3 are both
474 identified to have GxE variation in NPQ induction, but neither are associated with
475 obvious candidate genes that may be directly or indirectly involved in NPQ.
476 Nevertheless, a previous GWAS investigating the effects of climate on flowering time
477 identified genes that would not have obviously been attributed to that pathway
478 (Tabas-Madrid et al., 2018). A similar situation may be apparent in this study, but
479 more research is required.
480
481 NPQ is an extremely important physiological pathway that allows plants to adapt to
482 fluctuating lighting conditions and is therefore strongly influenced by the local
483 environment. Examples of adaptations that result from such environmental pressures
484 include the apparent increased reliance on the mechanism of the PsbS protein. This
485 study has also shown there are several genetic components to NPQ identified by
486 GWAS across simulated environments. Furthermore, there is evidence for a
487 significant genomic event that directly impacts PsbS expression and subsequently
488 impacts NPQ competence. In the face of current global climate challenges, better
489 understanding of the NPQ pathway could have important implications for agriculture
490 (Kromdijk et al., 2016) and may help better implement genomics-based strategies for
491 food security and conservation efforts.

ACKNOWLEDGEMENTS

This work was supported by grants from the ARC centre of excellence in Plant Energy Biology and the Australian National University for TR, AA, RC, PW, JO and BP and also for providing publication cost. The Australian Plant Phenomics Facility is supported under the National Collaborative Research Infrastructure Strategy of the Australian Government. TS is supported by the Jean Rogerson Postgraduate Scholarship. PG and E-MA acknowledge support from Academy of Finland projects 26080341, 307335 and 303757.

FIGURES

Table 1. Plants were grown in climatic growth chambers programmed to simulate the daily temperature ranges for late- and early-autumn conditions historically found in Australian coastal and inland environments. Temperature ranges gradually changed over time during the course of the experiments.

Table 2. Fifteen QTL were identified for NPQ and other photosynthetic traits across four conditions and two developmental stages. The component of NPQ found to be associated with the specified QTL are listed under the conditions they were identified (colour-coded for convenience). G x E – genotype-by-environment interaction; [e] analysis results at 14-leaf stage; [f] analysis results at 16-leaf stage

Figure 1: Natural variation of growth in response to different environmental conditions of 284 Arabidopsis accessions and 2 photoprotective mutants (*npq1*, *npq4*) within coastal (A) and inland (B) conditions. In this experiment, plants were

517 measured for NPQ when Col-0 control plants (red boxes) reached the 16-leaf stage
518 in both growth conditions to minimise developmental effects. (C – F) NPQ kinetic
519 profiles of 14-leaf plants grown in early (C) and late (D) autumn conditions and 16-
520 leaf plants grown in early (E) and late (F) autumn conditions.
521
522 **Figure 2**: (A) NPQ kinetics profile of 16-leaf plants grown in late autumn conditions
523 highlighting the key components of NPQ that were the focus of GWAS analysis. (B-
524 J) Results of GWAS performed during the three stages of NPQ defined in (A) on
525 plants grown in coastal late-autumn (B-D) and inland late-autumn (E-G) conditions,
526 as well as Gene x Environment interactions (H-J) with the most significant SNPs
527 highlighted. The dotted lines indicate the Bonferroni threshold of significance.
528
529 **Figure 3**: Association of SNPs in the region of QTL1-4, a QTL found to be significant
530 during both the NPQ steady and relaxation phases for plants grown in coastal late-
531 autumn conditions. The more significant SNPs are concentrated within the promoter
532 region of the *PSBS* gene (AT1G44575). The black dotted lines indicate the
533 Bonferroni threshold of significance.
534
535 **Figure 4**: (A-D) Coverage tracks of the *PSBS* genomic regions from five low NPQ (A
536 and B) and five high NPQ (C and D) Arabidopsis accessions aligned with the TAIR
537 10 Col-0 reference genome (low NPQ accession; A and C) and KBS-Mac-74
538 genome (high NPQ accession; B and D). Values along x-axes indicate the base pair
539 distance relative to the *PSBS* transcription start site. Genes along the track are
540 coloured green and the intergenic region is coloured pink. (E) Graphical view of the
541 alignment of the TAIR 10 Col-0 and the KBS-Mac-74 *PSBS* genomic regions. Axis

542 values refer to base pair positions within the respective tracks. (F) Comparison of the
543 average relative PsbS protein abundance between low and high NPQ accessions.
544 Error bars represent standard deviations. N=30; *** P < 0.001 with paired Student's
545 T test.
546
547 **REFERENCES**

548 Alsharafa, K., Vogel, M. O., Oelze, M.-L., Moore, M., Stingl, N., König, K., . . . Dietz,
549 K.-J. (2014). Kinetics of retrograde signalling initiation in the high light
550 response of Arabidopsis thaliana. *Phil. Trans. R. Soc. B, 369*(1640),
551 20130424.
552 Bolger, A. M., Lohse, M., & Usadel, B. (2014). Trimmomatic: a flexible trimmer for
553 Illumina sequence data. *Bioinformatics, 30*(15), 2114-2120.
554 doi:10.1093/bioinformatics/btu170
555 Bölter, B., Seiler, F., Soll, J. (2018). Analysis of *Arabidopsis thaliana* Growth
556 Behavior in Different Light Qualities. *J. Vis. Exp.* (132), e57152,
557 doi:10.3791/57152.
558 Briantais, J. M., Vernotte, C., Picaud, M., & Krause, G. H. (1979). Quantitative Study
559 of the Slow Decline of Chlorophyll Alpha-Fluorescence in Isolated-
560 Chloroplasts. *Biochimica Et Biophysica Acta, 548*(1), 128-138. doi:Doi
561 10.1016/0005-2728(79)90193-2
562 Brown, T. B., Cheng, R. Y., Sirault, X. R. R., Rungrat, T., Murray, K. D., Trtilek, M., . .
563 . Borevitz, J. O. (2014). TraitCapture: genomic and environment modelling of
564 plant phenomic data. *Current Opinion in Plant Biology, 18*, 73-79.
565 doi:10.1016/j.pbi.2014.02.002

566 Cheng, R., Abney, M., Palmer, A. A., & Skol, A. D. (2011). QTLRel: an R Package
567 for Genome-wide Association Studies in which Relatedness is a Concern.
568 *Bmc Genetics, 12*. doi:10.1186/1471-2156-12-66
569 Cheng, R., Parker, C. C., Abney, M., & Palmer, A. A. (2013). Practical considerations
570 regarding the use of genotype and pedigree data to model relatedness in the
571 context of genome-wide association studies. *G3: Genes, Genomes, Genetics*,
572 g3. 113.007948.
573 1001 Genomes Consortiom (2016). 1,135 Genomes Reveal the Global Pattern of
574 Polymorphism in Arabidopsis thaliana. *Cell, 166*(2), 481-491.
575 doi:10.1016/j.cell.2016.05.063
576 Correa-Galvis, V., Poschmann, G., Melzer, M., Stuhler, K., & Jahns, P. (2016). PsbS
577 interactions involved in the activation of energy dissipation in Arabidopsis.
578 *Nature Plants, 2*(2). doi:10.1038/Nplants.2015.225
579 Demmig-Adams, B., & Adams, W. W. (1992). Photoprotection and Other Responses
580 of Plants to High Light Stress. *Annual Review of Plant Physiology and Plant*
581 *Molecular Biology, 43*, 599-626. doi:DOI
582 10.1146/annurev.pp.43.060192.003123
583 Hedden, P., & Sponsel, V. (2015). A century of gibberellin research. *Journal of plant*
584 *growth regulation, 34*(4), 740-760.
585 Herritt, M., Dhanapal, A. P., & Fritschi, F. B. (2016). Identification of Genomic Loci
586 Associated with the Photochemical Reflectance Index by Genome-Wide
587 Association Study in Soybean. *Plant Genome, 9*(2).
588 doi:10.3835/plantgenome2015.08.0072

589 Horton, P., Wentworth, M., & Ruban, A. (2005). Control of the light harvesting
590 function of chloroplast membranes: The LHCII-aggregation model for non-
591 photochemical quenching. *Febs Letters, 579*(20), 4201-4206.
592 Huala, E., Dickerman, A. W., Garcia-Hernandez, M., Weems, D., Reiser, L., LaFond,
593 F., . . . Huang, W. (2001). The Arabidopsis Information Resource (TAIR): a
594 comprehensive database and web-based information retrieval, analysis, and
595 visualization system for a model plant. *Nucleic Acids Research, 29*(1), 102-
596 105.
597 Ishida, S., Takabayashi, A., Ishikawa, N., Hano, Y., Endo, T., & Sato, F. (2009). A
598 novel nuclear-encoded protein, NDH-dependent cyclic electron flow 5, is
599 essential for the accumulation of chloroplast NAD (P) H dehydrogenase
600 complexes. *Plant and cell physiology, 50*(2), 383-393.
601 Jahns, P., & Holzwarth, A. R. (2012). The role of the xanthophyll cycle and of lutein
602 in photoprotection of photosystem II. *Biochimica et Biophysica Acta (BBA)-*
603 *Bioenergetics, 1817*(1), 182-193.
604 Jung, H. S., & Niyogi, K. K. (2009). Quantitative Genetic Analysis of Thermal
605 Dissipation in Arabidopsis. *Plant Physiology, 150*(2), 977-986.
606 doi:10.1104/pp.109.137828
607 Kromdijk, J., Glowacka, K., Leonelli, L., Gabilly, S. T., Iwai, M., Niyogi, K. K., & Long,
608 S. P. (2016). Improving photosynthesis and crop productivity by accelerating
609 recovery from photoprotection. *Science, 354*(6314), 857-861.
610 doi:10.1126/science.aai8878
611 Langmead, B., & Salzberg, S. L. (2012). Fast gapped-read alignment with Bowtie 2.
612 *Nature Methods, 9*(4), 357-U354. doi:10.1038/Nmeth.1923

613 Li, Y., Cheng, R., Spokas, K.A., Palmer, A.A., & Borevitz, J.O. (2014). Genetic
614 Variation for Life History Sensitivity to Seasonal Warming in Arabidopsis
615 thaliana. *Genetics,* 196(2): 569-577
616 Li, H., Handsaker, B., Wysoker, A., Fennell, T., Ruan, J., Homer, N., . . . Proc, G. P.
617 D. (2009). The Sequence Alignment/Map format and SAMtools.
618 *Bioinformatics, 25*(16), 2078-2079. doi:10.1093/bioinformatics/btp352
619 Li, X. P., Bjorkman, O., Shih, C., Grossman, A. R., Rosenquist, M., Jansson, S., &
620 Niyogi, K. K. (2000). A pigment-binding protein essential for regulation of
621 photosynthetic light harvesting. *Nature, 403*(6768), 391-395. doi:Doi
622 10.1038/35000131
623 Li, X. P., Gilmore, A. M., Caffarri, S., Bassi, R., Golan, T., Kramer, D., & Niyogi, K. K.
624 (2004). Regulation of photosynthetic light harvesting involves intrathylakoid
625 lumen pH sensing by the PsbS protein. *Journal of Biological Chemistry,*
626 *279*(22), 22866-22874. doi:10.1074/jbc.M402461200
627 Li, Y., Huang, Y., Bergelson, J., Nordborg, M., & Borevitz, J. O. (2010). Association
628 mapping of local climate-sensitive quantitative trait loci in Arabidopsis
629 thaliana. *Proceedings of the National Academy of Sciences of the United*
630 *States of America, 107*(49), 21199-21204. doi:10.1073/pnas.1007431107
631 Listgarten, J., Lippert, C., Kadie, C. M., Davidson, R. I., Eskin, E., & Heckerman, D.
632 (2012). Improved linear mixed models for genome-wide association studies.
633 *Nature Methods, 9*(6), 525.
634 Lohmeier-Vogel, E. M., Kerk, D., Nimick, M., Wrobel, S., Vickerman, L., Muench, D.
635 G., & Moorhead, G. B. (2008). Arabidopsis At5g39790 encodes a chloroplast-
636 localized, carbohydrate-binding, coiled-coil domain-containing putative
637 scaffold protein. *BMC Plant Biology, 8*(1), 120.

638 Michael, T. P., Jupe, F., Bemm, F., Motley, S. T., Sandoval, J. P., Lanz, C., . . .
639 Ecker, J. R. (2018). High contiguity Arabidopsis thaliana genome assembly
640 with a single nanopore flow cell. *Nature communications, 9*(1), 541.
641 Niyogi, K. K., Grossman, A. R., & Bjorkman, O. (1998). Arabidopsis mutants define a
642 central role for the xanthophyll cycle in the regulation of photosynthetic energy
643 conversion. *Plant Cell, 10*(7), 1121-1134. doi:DOI 10.1105/tpc.10.7.1121
644 Potter, T. I., Rood, S. B., & Zanewich, K. P. (1999). Light intensity, gibberellin
645 content and the resolution of shoot growth in Brassica. *Planta, 207*(4), 505-
646 511.
647 Priyam, A., Woodcroft, B. J., Rai, V., Munagala, A., Moghul, I., Ter, F., . . . Rumpf,
648 W. (2015). Sequenceserver: a modern graphical user interface for custom
649 BLAST databases. *bioRxiv*, 033142.
650 Quinlan, A. R., & Hall, I. M. (2010). BEDTools: a flexible suite of utilities for
651 comparing genomic features. *Bioinformatics, 26*(6), 841-842.
652 doi:10.1093/bioinformatics/btq033
653 Ramirez, F., Ryan, D. P., Gruning, B., Bhardwaj, V., Kilpert, F., Richter, A. S., . . .
654 Manke, T. (2016). deepTools2: a next generation web server for deep-
655 sequencing data analysis. *Nucleic Acids Research, 44*(W1), W160-W165.
656 doi:10.1093/nar/gkw257
657 Rousseau, C., Belin, E., Bove, E., Rousseau, D., Fabre, F., Berruyer, R., . . .
658 Boureau, T. (2013). High throughput quantitative phenotyping of plant
659 resistance using chlorophyll fluorescence image analysis. *Plant Methods,*
660 *9*(1), 17.

661 Ruban, A. V. (2016). Nonphotochemical Chlorophyll Fluorescence Quenching:
662 Mechanism and Effectiveness in Protecting Plants from Photodamage. *Plant*
663 *Physiology, 170*(4), 1903-1916. doi:10.1104/pp.15.01935
664 Rungrat, T., Awlia, M., Brown, T., Cheng, R., Sirault, X., Fajkus, J., . . . Tester, M.
665 (2016). Using phenomic analysis of photosynthetic function for abiotic stress
666 response gene discovery. *The Arabidopsis Book*, e0185.
667 Spokas, K., & Forcella, F. (2006). Estimating hourly incoming solar radiation from
668 limited meteorological data. *Weed Science, 54*(1), 182-189. doi:Doi
669 10.1614/Ws-05-098r.1
670 Stowe, B. B., & Yamaki, T. (1957). The history and physiological action of the
671 gibberellins. *Annual review of plant physiology, 8*(1), 181-216.
672 Tabas-Madrid, D., Méndez-Vigo, B., Arteaga, N., Marcer, A., Pascual-Montano, A.,
673 Weigel, D., . . . Alonso-Blanco, C. (2018). Genome-wide signatures of
674 flowering adaptation to climate temperature: Regional analyses in a highly
675 diverse native range of Arabidopsis thaliana. *Plant, cell & environment*.
676 van Rooijen, R., Aarts, M. G., & Harbinson, J. (2015). Natural genetic variation for
677 acclimation of photosynthetic light use efficiency to growth irradiance in
678 Arabidopsis. *Plant Physiology, 167*(4), 1412-1429.
679 Wang, Q. X., Zhao, H., Jiang, J. P., Xu, J. Y., Xie, W. B., Fu, X. K., . . . Wang, G. W.
680 (2017). Genetic Architecture of Natural Variation in Rice Nonphotochemical
681 Quenching Capacity Revealed by Genome-Wide Association Study. *Frontiers*
682 *in Plant Science, 8*. doi:10.3389/fpls.2017.01773
683 Weigel, D., & Mott, R. (2009). The 1001 genomes project for Arabidopsis thaliana.
684 *Genome biology, 10*(5), 107.

685 Wintersinger, J. A., & Wasmuth, J. D. (2015). Kablammo: an interactive, web-based
686 BLAST results visualizer. *Bioinformatics, 31*(8), 1305-1306.
687 doi:10.1093/bioinformatics/btu808
688 Zhang, X., Hause, R. J., & Borevitz, J. O. (2012). Natural Genetic Variation for
689 Growth and Development Revealed by High-Throughput Phenotyping in
690 Arabidopsis thaliana. *G3-Genes Genomes Genetics, 2*(1), 29-34.
691 doi:10.1534/g3.111.001487

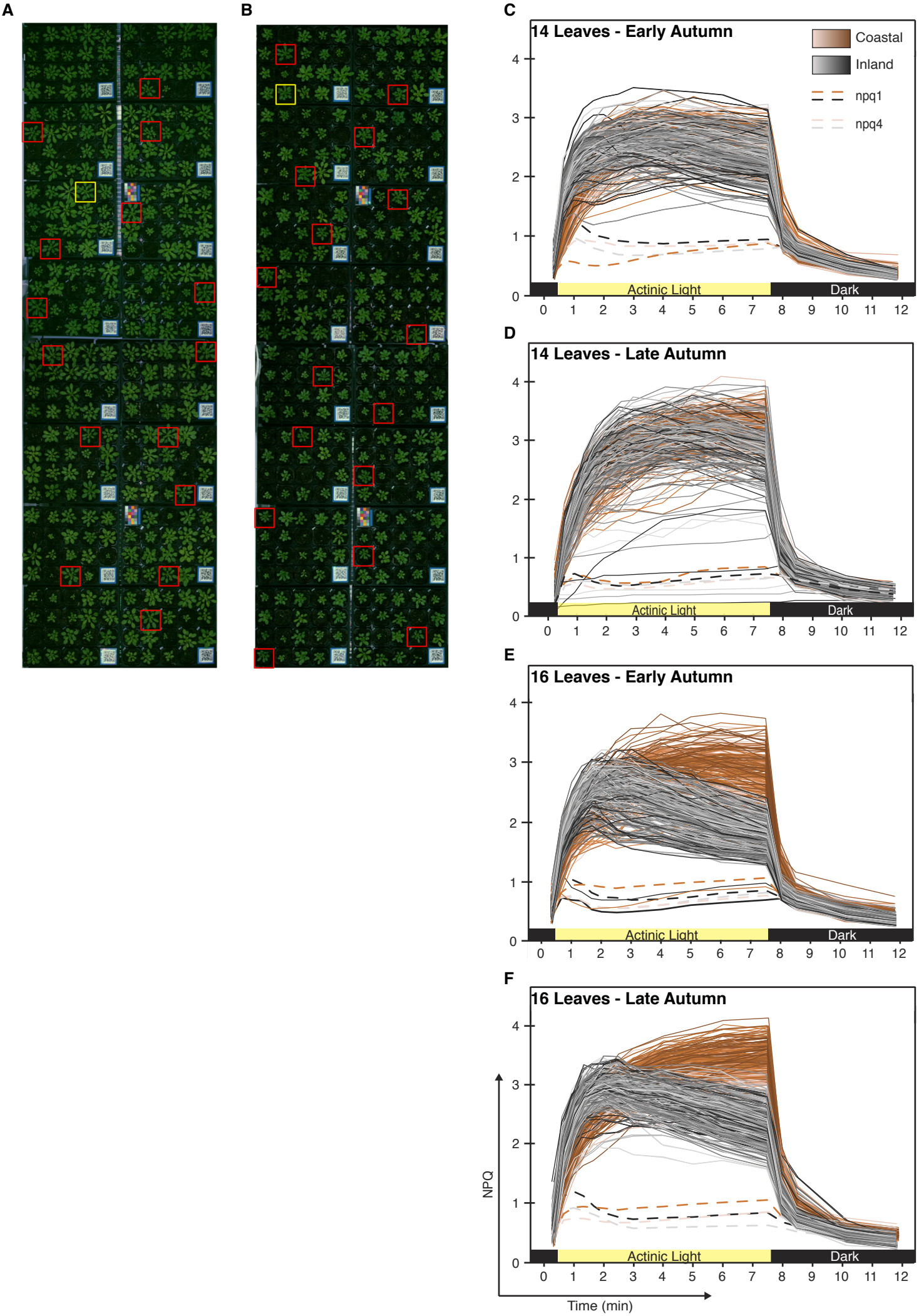

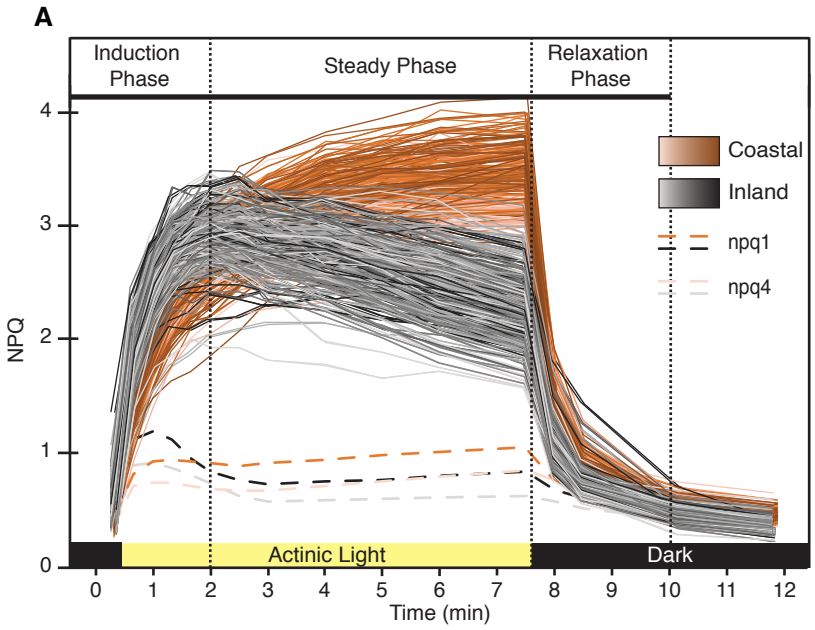

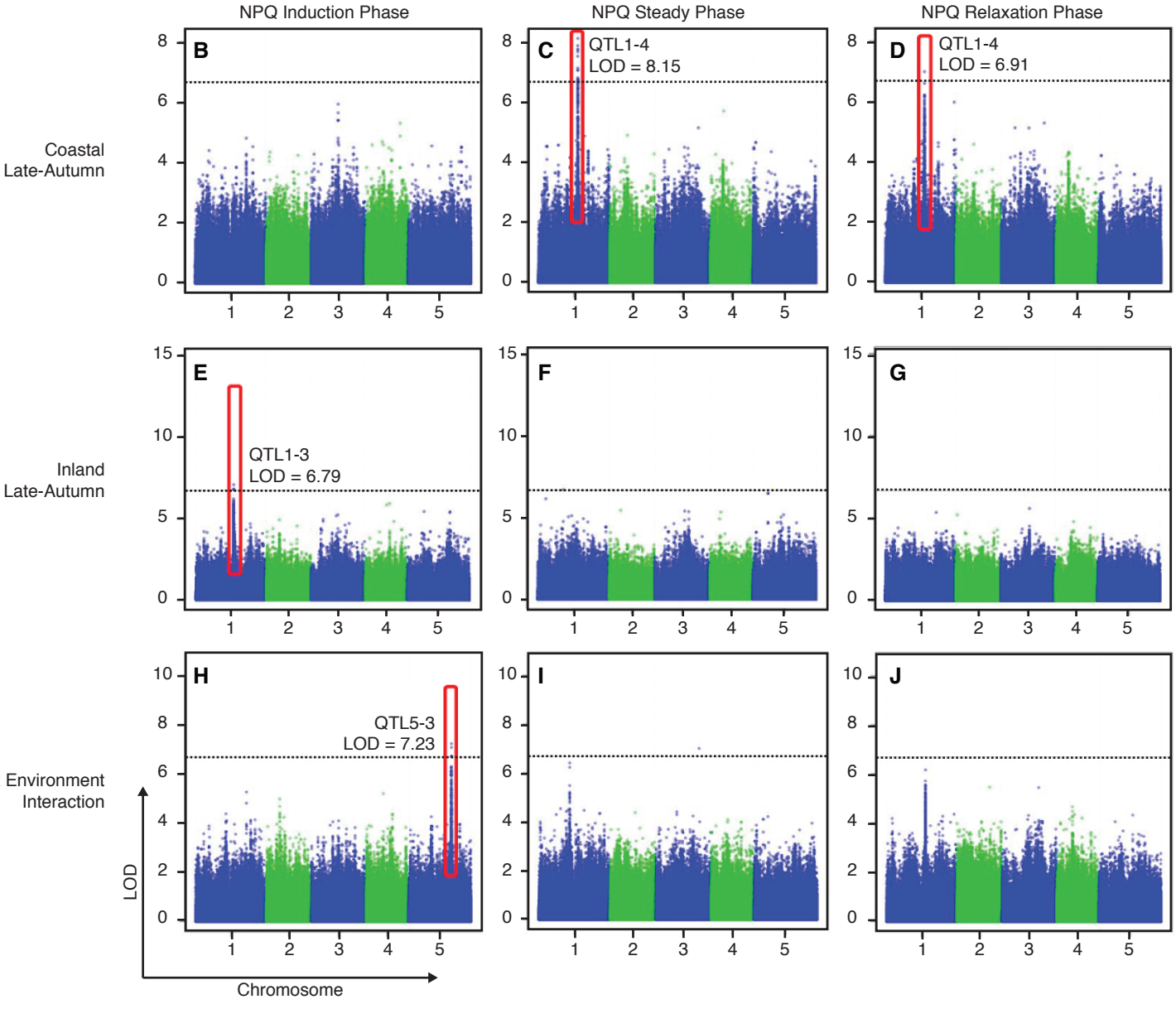

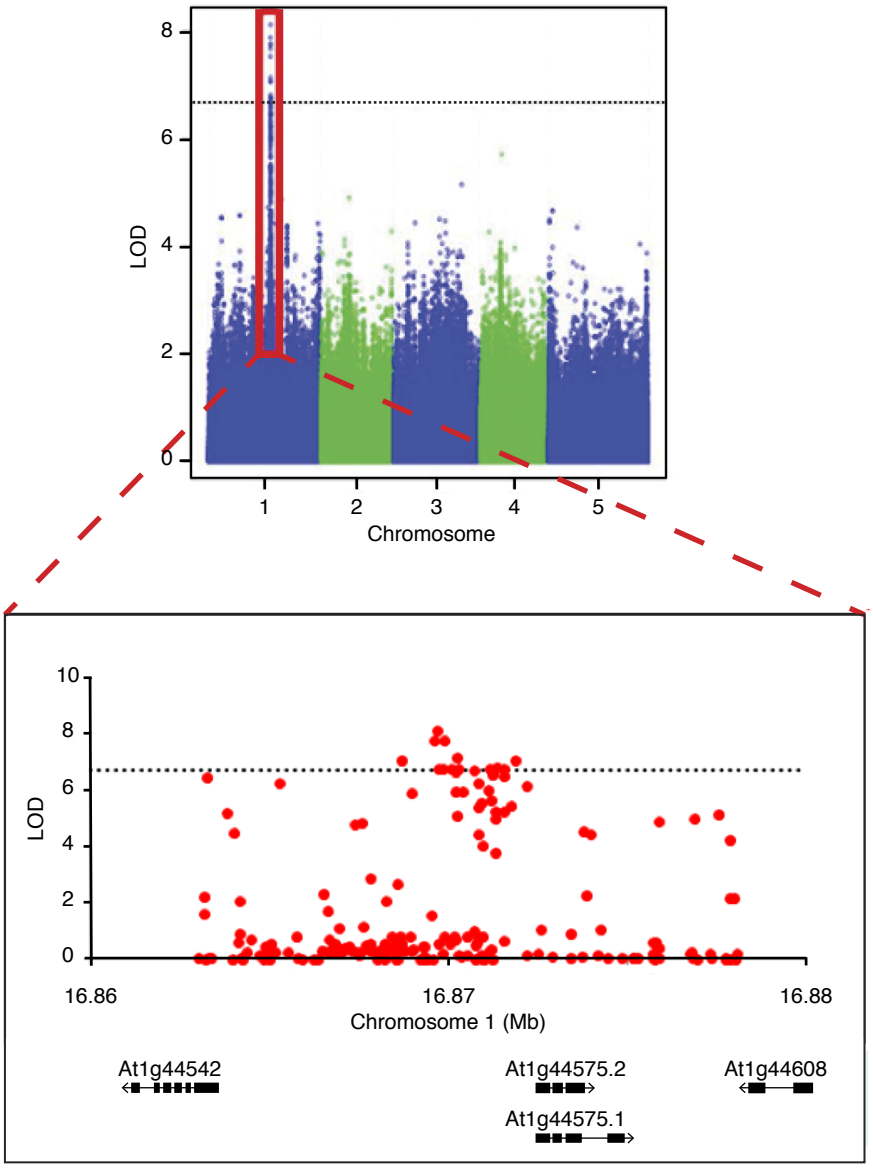

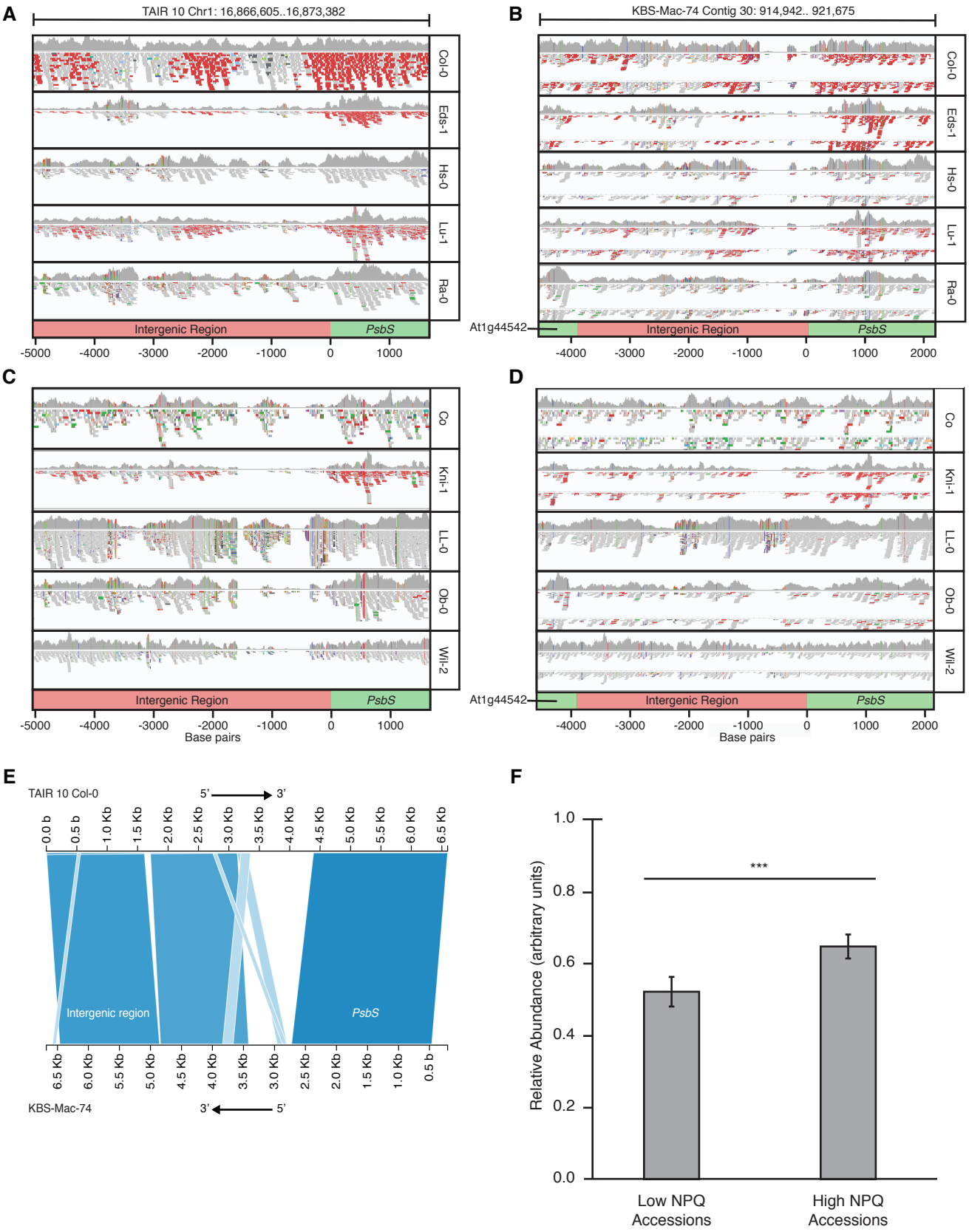

Environment	Maximum light intensity at noon ($\mu mol\ m^{-2}\ s^{-1}$)	Simulated seasons and dates	Temperature range	
			Beginning	End
Coastal	150	Early Autumn | 15 Mar 2015 - 7 May 2015	14 - 24˚C	10 - 20˚C
		Late Autumn | 1 Apr 2014 - 5 Jun 2014	13 - 23˚C	5 - 14˚C
Inland	300	Early Autumn | 15 Mar 2015 - 7 May 2015	11 - 24˚C	6 - 18˚C
		Late Autumn | 1 Apr 2014 - 5 Jun 2014	10 - 23˚C	5 - 14˚C

QTL	Chr	Position (bp)	LOD score	Col-0 allele Frequency	% variation explained	Trait appearance					
						Late Autumn			Early Autumn		
						Coastal	Inland	G x E	Coastal	Inland	G x E
QTL1-1	1	349 233	8.66	0.24	3.4	NPQ Steady [e]					
QTL1-2	1	9 729 376	7.04	0.36	9.2				F_V'/F_m' [f]		
QTL1-3	1	16 351 441	7.04	0.52	5.6		NPQ Slope Induction [f]				
QTL1-4	1	16 869 695	8.15	0.79	9.5	F_V'/F_m' [f]	QY-max [f]				
						NPQ Steady [f]					
						NPQ Max [f]					
						NPQ Slope Relaxation [f]					
QTL1-5	1	20 680 932	7.93	0.05	13.7					NPQ Steady [f]	
QTL2-1	2	10 934 450	8.07	0.07	10.1		F_V'/F_m' [f]				
QTL2-2	2	10 984 417	7.95	0.06	12.2		NPQ Steady [e]				
							QY-max [f]				
QTL2-3	2	11 680 235	7.00	0.21	6.7						NPQ Slope Induction [f]
QTL4-1	4	1 509 645	7.95	0.19	0.9					F_V'/F_m' [f]	F_V'/F_m' [f]
QTL4-2	4	5 270 810	7.14	0.22	7.5					NPQ Slope Induction [f]	
QTL4-3	4	13 911 309	9.13	0.06	0.1				NPQ Steady [e]		
QTL5-1	5	15 037 793	6.93	0.09	1.4	NPQ Relaxation [f]					
QTL5-2	5	15 930 795	7.27	0.22	11.7					NPQ Relaxation [f]	
QTL5-3	5	18 511 604	7.23	0.26	2.3			NPQ Slope Induction [f]			
QTL5-4	5	25 477 423	7.71	0.11	14.0				NPQ Steady [f]		